Journal of Applied Sciences

ISSN 1812-5654

Journal of Applied Sciences 7 (4): 553-558, 2007
ISSN 1812-5654

Application of Central Difference Scheme to the Solution of Natural Convection Equations for Irregular Shaped Enclosures

[1]Yasin Varol, [2]Ahmet Koca and [3]Hakan F. Oztop
[1]Department of Mechanical Engineering, Vanderbilt University, Nashville, TN 37235, USA
[2]Department of Mechanical Science, Firat University, TR-23119, Elazig, Turkey
[3]Department of Mechanical Engineering, Firat University, TR-23119, Elazig, Turkey

Abstract: The present study deals with the numerical solution of laminar natural convection equations for irregular shaped enclosure using Central Difference Scheme (CDS). Governing equations in streamfunction-vorticity form were discretized over a grid arrangement. A code was developed using an algorithm. Successive Under Relaxation (SUR) method was used to solve algebraic equations. Two different geometries were chosen as illustrative examples such as triangular and irregular shaped enclosures whose bottom wall was isothermally cooled and inclined walls were isothermally heated. The obtained results were compared with different techniques which are available from the literature. The obtained results show good agreement between literature and the present data.

Key words: Natural convection, irregular shape, computational modeling, central difference

INTRODUCTION

Solutions of Navier-Stokes equations with or without buoyancy terms for regular shaped geometries such as square or rectangle are studied widely in the open literature due to their wide applications and simplicity of the solution (Ostrach, 1988; Gebhart *et al*., 1988; De Vahl Davis and Jones, 1983). In these geometries, nodes are coincide with the boundaries of the geometry. However, the analysis of natural convection heat transfer in irregular geometries is more complex due to complexity of the geometry. Thus, it is difficult to analyze the flow both mathematically and physically.

Natural convection heat transfer and fluid flow in irregular geometries also wide application area. The geometries can be irregular shapes due to construction necessities. To analyze the natural convection in those geometries, some numerical techniques are developed especially on grid generation, such as conformal mapping, elliptic grid generation, simple coordinate transformation technique, orthogonal mapping, transfinite interpolation method, hyperbolic grid generation etc. (Knupp and Steinberg, 1994; Oztop, 2003; Thames *et al*., 1977).

Moukalled and Acharya (2001) made a numerical study to analyze the conjugate natural convection in a trapezoidal enclosure using finite volume method. Grid generation is obtained by transfinite interpolation technique. Akinsete and Coleman (1982) analyzed the natural convection heat transfer in a triangular enclosure using finite difference technique. The analyses performed for the same geometry by Asan and Namli (2000, 2001), Tzeng *et al*. (2005) and Kent *et al*. (2005). They used the finite volume method to solve natural convection in triangular cross-sectional enclosure for different boundary conditions such as summerlike (ceiling is hot, bottom is cold) and winterlike (ceiling is cold, bottom is hot). However, Tzeng *et al*. (2005) applied the NSPA technique for solution of governing equations of laminar natural convection in triangular enclosure for different boundary conditions. Kent *et al*. (2005) solved natural convection equations using Galerkin-finite element method for the triangular enclosure and they showed the flow and temperature distribution. For the same geometry, Holtzman *et al*. (2000) applied the non-symmetric boundary conditions using FIDAP commercial code and Karyakin *et al*. (1988) solved the same problem for transient regime with finite difference method and MAC cell.

Morsi and Das (2003) performed a study for complex shaped enclosures such as flat, inclined and dome shaped. They used the finite element method to obtain the mathematical domain. They indicated that the convective phenomenon strongly influenced by the shape of dome with the same Rayleigh number. Correa (1987) solved natural convection heat transfer in an incandescent lamps using body-fitted computational grid. They analyzed the different type (geometry) of lamps (i.e., vertical and horizontal lamps).

Corresponding Author: Yasin Varol, Department of Mechanical Engineering, Vanderbilt University, Nashville, TN 37235, USA
Tel: +1615419-2734 Fax: +1615343-6687

The main aim of this study is to show the effectiveness and simplicity of central-difference scheme on solving of differential equations of natural convection in irregular geometries. The literature shows that studies on natural convection in irregular shaped geometries are very limited. Thus, this paper proposes a simple technique to investigate the natural convection problem. Two illustrative examples are presented as triangular cross-section geometry which is used to test the present code and irregular shaped geometry.

Solution methodology: Laminar two-dimensional Navier-Stokes equations in streamfunction-vorticity form is written as Eqs. (1-3) for steady, two-dimensional, incompressible, Newtonian fluid with Boussinesq approximation (Gray and Giorgini, 1976).

$$-\Omega = \frac{\partial^2\Psi}{\partial X^2} + \frac{\partial^2\Psi}{\partial Y^2} \tag{1}$$

$$\frac{\partial^2\Omega}{\partial X^2} + \frac{\partial^2\Omega}{\partial Y^2} = \frac{1}{Pr}\left(\frac{\partial\Psi}{\partial Y}\frac{\partial\Omega}{\partial X} - \frac{\partial\Psi}{\partial X}\frac{\partial\Omega}{\partial Y}\right) - Ra\left(\frac{\partial\theta}{\partial X}\right) \tag{2}$$

$$\frac{\partial^2\theta}{\partial X^2} + \frac{\partial^2\theta}{\partial Y^2} = \frac{\partial\Psi}{\partial Y}\frac{\partial\theta}{\partial X} - \frac{\partial\Psi}{\partial X}\frac{\partial\theta}{\partial Y} \tag{3}$$

Based on the Non-dimensional variables are given as

$$X = \frac{x}{L}, \quad Y = \frac{y}{L}, \Psi = \frac{\psi Pr}{\upsilon}, \quad \Omega = \frac{\omega(L)^2 Pr}{\upsilon}, \quad \theta = \frac{T - T_{cold}}{T_{hot} - T_{cold}} \tag{4}$$

$$u = \frac{\partial\psi}{\partial y}, \quad v = -\frac{\partial\psi}{\partial x}, \quad \omega = \left(\frac{\partial v}{\partial x} - \frac{\partial u}{\partial y}\right), \quad Ra = \frac{\beta g(T_{hot} - T_{cold})L^3 Pr}{\upsilon^2}, \quad Pr = \frac{\upsilon}{\alpha} \tag{5}$$

The flow chart has been shown in Fig. 1. It starts with input data and initial value. Streamfunction, vorticity and temperatures are calculated by solving algebraic equations. After than the necessary values such as Nusselt number, pressure is calculated. If a convergence criterion is obtained, the output file is printed. Otherwise, it goes to starting point. Schematic of grid arrangement is given in Fig. 2. Discretization is performed according to this grid arrangement. Eq. 6 gives the discretization of continuity equation (Eq. 1) as

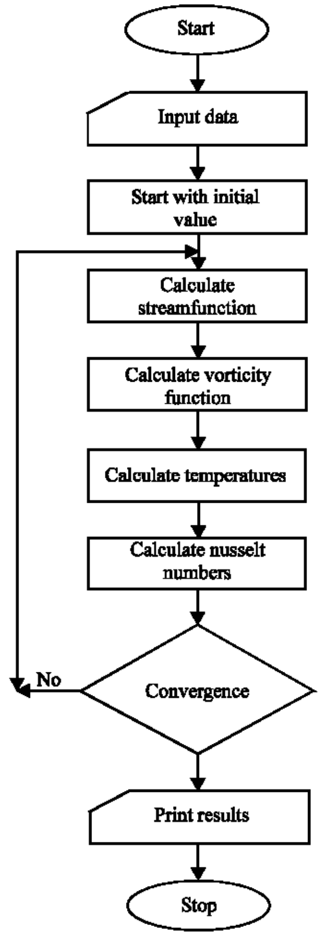

Fig. 1: Flow chart for the code

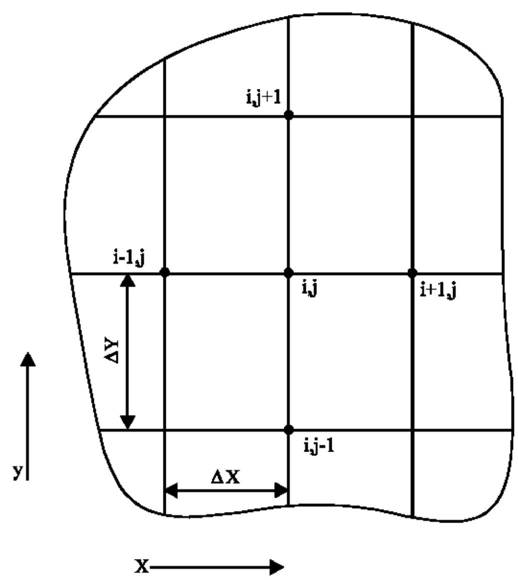

Fig. 2: Grid arrangement

$$-\Omega_{i,j} = \frac{\Psi_{i+1,j} + \Psi_{i-1,j} - 2\Psi_{i,j}}{\Delta X^2} + \frac{\Psi_{i,j+1} + \Psi_{i,j-1} - 2\Psi_{i,j}}{\Delta Y^2} \quad (6)$$

and streamfunction is obtained

$$\Psi_{i,j} = \frac{\left[\left(\frac{\Psi_{i+1,j} + \Psi_{i-1,j}}{\Delta X^2}\right) + \left(\frac{\Psi_{i,j+1} + \Psi_{i,j-1}}{\Delta Y^2}\right)\right] + \Omega_{i,j}}{\left(\frac{2}{\Delta X^2} + \frac{2}{\Delta Y^2}\right)} \quad (7)$$

After the discretization of Eq. 2, vorticity is found as

$$\Omega_{i,j} = \left\{ \left(\frac{-1}{4\Delta X \Delta Y \, Pr}\right) \left[\left(\Psi_{i,j+1} - \Psi_{i,j-1}\right)\left(\Omega_{i+1,j} - \Omega_{i-1,j}\right) - \left(\Psi_{i+1,j} - \Psi_{i-1,j}\right)\left(\Omega_{i,j+1} - \Omega_{i,j-1}\right) \right] + \left(\frac{\Omega_{i+1,j} + \Omega_{i-1,j}}{\Delta X^2}\right) + \left(\frac{\Omega_{i,j+1} + \Omega_{i,j-1}}{\Delta Y^2}\right) - Ra\left(\frac{\theta_{i+1,j} - \theta_{i-1,j}}{2\Delta X}\right) \right\} \Big/ \left(\frac{2}{\Delta X^2} + \frac{2}{\Delta Y^2}\right) \quad (8)$$

Finally, temperature is obtained with discretization of energy equation (Eq. 3),

$$\theta_{i,j} = \left\{ \left(\frac{-1}{4\Delta X \Delta Y}\right) \left[\left(\Psi_{i,j+1} - \Psi_{i,j-1}\right)\left(\theta_{i+1,j} - \theta_{i-1,j}\right) - \left(\Psi_{i+1,j} - \Psi_{i-1,j}\right)\left(\theta_{i,j+1} - \theta_{i,j-1}\right) \right] + \left(\frac{\theta_{i+1,j} + \theta_{i-1,j}}{\Delta X^2}\right) + \left(\frac{\theta_{i,j+1} + \theta_{i,j-1}}{\Delta Y^2}\right) \right\} \Big/ \left(\frac{2}{\Delta X^2} + \frac{2}{\Delta Y^2}\right) \quad (9)$$

In these equations, ΔX and ΔY show grid distance as indicated in Fig. 2. Due to using of regular grid their value taken as $\Delta X = \Delta Y$.

Calculation of local Nusselt number using the following equation

$$Nu = -\left.\frac{\partial \theta}{\partial Y}\right|_{y=0} \quad (10)$$

Local or mean Nusselt number is obtained via Simpson integration rule as

$$da = \frac{\Delta n}{3}\left[f(x_{k+1}) + 4.f(x_k) + f(x_{k-1})\right] \quad (11)$$

Using this rule mean Nusselt number can be calculated as

$$Nu_m = \frac{\Delta x}{3}(Nu_{i,j} + 4Nu_{i+1,j} + 2Nu_{i+2,j} + 4Nu_{i+3,j} + 2Nu_{i+4,j} \; .....) \quad (12)$$

Mean Nusselt number for system is calculated with the arithmetical mean of both bottom and ceiling Nusselt numbers. Here, i and j are shown schematically in Fig. 2.

The computational results are validated against the results of Asan and Namli's study (2000) which used the triangular cross-sectional geometry to check accuracy of the code. Finite volume method was performed in their case. Akinsete and Coleman (1982) was used the finite different technique for the same problem. Recently, Tzeng *et al.* (2005) applied the NSPA technique to solve natural convection problem in a triangular enclosure. The obtained results of local Nusselt number was compared with that three studies at the same boundary conditions, Rayleigh number, Ra = 2772 and Prandtl number, Pr = 0.71 as can be seen from Fig. 3. The local Nusselt number was increased asymptotically with along the bottom wall. Also, the Nusselt number was very high at the intersection of hot and cold boundary due to high temperature difference. Thus, their value did not show up in the figure.

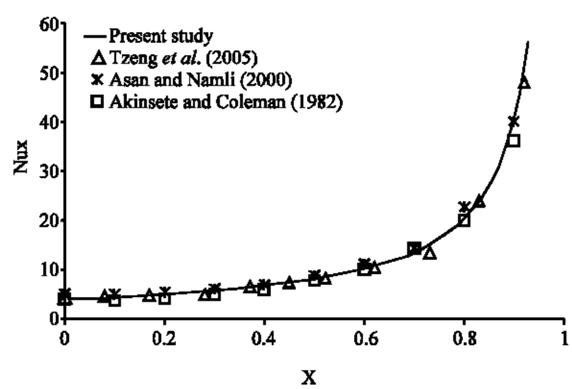

Fig. 3: Comparison of local Nusselt numbers for triangular geometry with literature

Governing equations in streamfunction-vorticity form (Eq. 1-3) were solved using central difference method. Algebraic equations were obtained via Taylor series and they solved with Successive Under Relaxation (SUR) technique, iteratively, which is defined in Eq. 13.

$$\phi^1 = \phi^0 + r.\left(\phi^{calculated} - \phi^0\right) \tag{13}$$

In this equation, ϕ is any variable and ϕ^0 and $\phi^{calculated}$ are the old value and calculated value of variable. However, ϕ^1 is the value for next step and r shows the relaxation factor whose value is less than 1. In the code, different relaxation parameters were chosen for θ, Ω and Ψ. The detailed solution technique is well described in the literature (Koca, 2005; Varol *et al*., 2007; Ozisik, 1994; Oosthuizen and Naylor, 1998). As a convergence criterion, 10^{-4} value is chosen for all depended variables.

Illustrative examples: Two different examples such as triangular and irregular shaped enclosures are shown to validation of the computational modeling. Triangular shaped enclosure is chosen to test the result with benchmark data.

Some grid dimensions were tested to obtain optimum grid dimension. To do this, several tests were conducted between grid dimensions of 35×35 and 215×215. It is decided that 145×145 and 121×121 grid dimensions were sufficiently fine to ensure a grid independent solution for triangular and irregular shaped geometries, respectively. Detailed variation of Nusselt number with grid dimension is given in Fig. 6 and related grid dimensions can be found in Table 1.

Illustrative example I: Figure 4 shows the physical and computational domain (left half) of the triangular geometry. Boundary conditions are also depicted Fig. 4. inclination angle is chosen as 18° for the case study. It is changeable according to other angles. Grid generation is obtained automatically. Other results are not shown to save space in the study. As indicated above, the triangular geometry is used to test the solution methodology and used algorithm. As boundary condition, bottom wall is chosen cold constant temperature while inclined surface is hot that is defined by Eq. 14-16. This boundary conditions refers to the summerlike boundary conditions for gable roofs. Symmetrical solution is performed for left half with length L and height H.

Table 1: Grid dimensions at different grid numbers

Grid No.	Grid dimensions
1	35×35
2	51×51
3	77×77
4	97×97
5	121×121
6	145×145
7	177×177
8	193×193
9	215×215

Illustrative example II: In this part of the present paper, natural convection heat transfer and fluid flow is analyzed in irregular shaped enclosure. A symmetrical solution performed for this more complex geometry. Boundary conditions are chosen as the same with triangular enclosure. Inclined part has different angles and can be change according to definition of boundary. Related physical model with dimension and coordinate is given in Fig. 5. It includes two parts of the grid arrangement to obtain smoothless grid disribution. Boundary conditions and grid arrangement also depicted on the Fig. 5.

Boundary conditions for above illustrative examples as given as follows:

On the inclined surfaces

$$u=v=0,\ T=T_{hot} \tag{14}$$

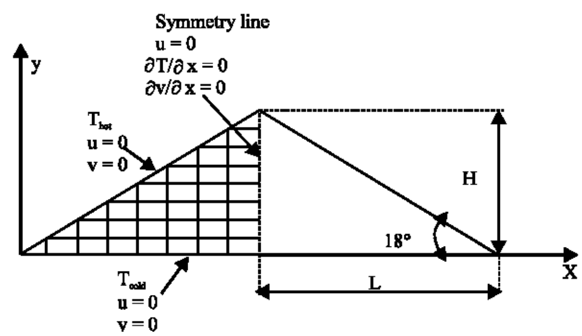

Fig. 4: Schematic of configuration and grid distribution for triangular geometry

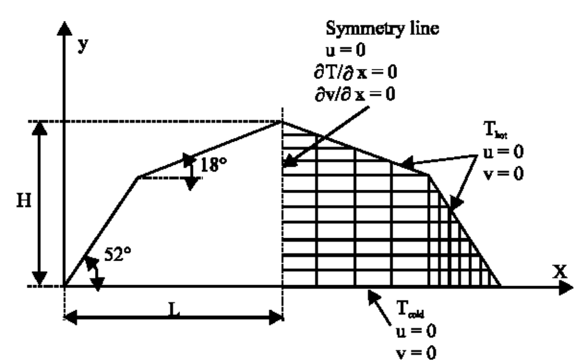

Fig. 5: Schematic of configuration and grid distribution for irregular shaped enclosure geometry

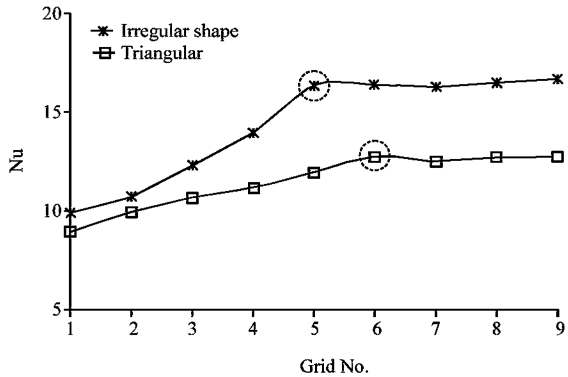

Fig. 6: Variation of mean Nusselt numbers with grid dimensions

On the bottom wall

$$u=v=0, T=T_{cold} \tag{15}$$

On the vertical wall

$$u=0, v=0, \frac{\partial T}{\partial x}=0 \tag{16}$$

RESULTS AND DISCUSSION

Results are presented for two test geometries in terms of streamlines, isotherms and mean Nusselt numbers. Figure 7a shows the streamline (on the left) and isotherm (on the right) for triangular geometry for Ra = 10^6. A single cell was obtained in the counterclockwise direction. Flow rate was increased near the inclined boundary because convection heat transfer was effective at that region. Thus, streamlines were stratified. Isotherms were plotted in Fig. 7a (on the right). Due to the top heating, intensification of temperature to the fluid was very low according to natural convection mechanism. They followed the boundaries until the mid-line of the triangular enclosure. Again, streamline (on the left) and isotherm (on the right) are shown in Fig. 7b for irregular geometry at Ra = 10^6. Due to symmetrical boundary conditions at the middle of the enclosure, a stagnation point was formed and flow behaves as jet impingement on to horizontal plate. Isotherms followed the boundaries and orthogonal to the symmetry axis. As indicated in the Fig. 8, mean Nusselt number was almost constant for all Rayleigh number because of the top heating and mechanism of natural convection. These results are supported by Asan and Namli (2000). However, mean Nusselt number increased after the value of Ra>10^4 for irregular shaped enclosure. Up to this value, conduction heat transfer mode was dominant to convection. For higher Ra number, it increased due to effect of convection dominant regime.

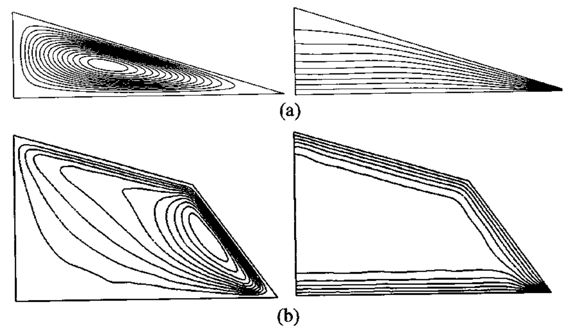

Fig. 7: Streamlines and isotherms for different geometry at Ra = 10^6, a) Triangular enclosure, b) Irregular shaped enclosure

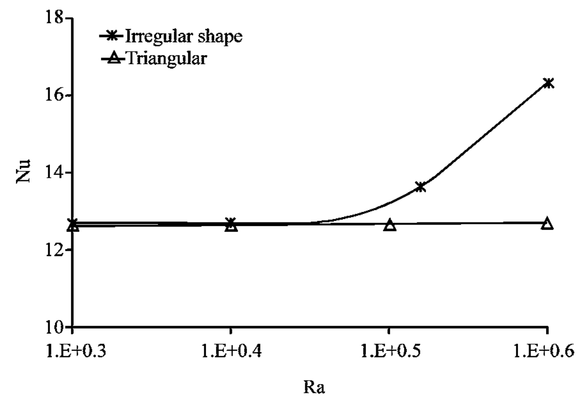

Fig. 8: Variation of mean Nusselt number with different Rayleigh numbers for irregular shaped enclosure

CONCLUSIONS

Natural convection heat transfer and flow field is performed for irregular shaped enclosures using central difference techniques. Two different illustrative examples are presented in the present study. The results for triangular geometry showed a good agreement with the earlier studies. However, the method was tested for more complex geometry for the same boundary conditions. A circulation cell was obtained in counterclockwise and a stagnation point was formed at the mid-line of the enclosure. Due to effectiveness of conduction mode of heat transfer, mean Nusselt number became constant with increasing Rayleigh number in triangular enclosure. However, it increased for Ra>10^4 since complexity of boundaries helped the acceleration of the flow.

Finally, the present study shows that the proposed computational model can be used to analyze the natural convection phenomena occurring irregular shaped enclosures. This study can be extended for higher Rayleigh number and more complex geometries.

NOMENCLATURE

g	Gravitational acceleration (m s^{-2})
Gr	Grashof number
L	Length of bottom wall (m)
i, j	Horizontal and vertical nodes
H	Maximum length of roof (m)
Nu	Nusselt number
Pr	Prandtl number
r	Relaxation function
Ra	Rayleigh number
T	Temperature (K)
u, v	Horizontal and vertical velocities (m s^{-1})
X, Y	Non-dimensional coordinates

GREEK LETTERS

ρ	Density (kg m^{-3})
υ	Kinematic viscosity (m^2 s^{-1})
θ	Non-dimensional temperature
Ω	Non-dimensional vorticity
β	Thermal expansion coefficient (K^{-1})
α	Thermal diffusivity (m^2 s^{-1})
Ψ	Non-dimensional streamfunction

REFERENCES

Akinsete, V. and T.A. Coleman, 1982. Heat transfer by steady laminar free convection in triangular enclosures. Int. J. Heat Mass Transfer, 25: 991-998.

Asan, H. and L. Namli, 2000. Laminar natural convection in a pitched roof of triangular cross-section: Summer day boundary conditions. Energy Buildings, 33: 69-73.

Asan, H. and L. Namli, 2001. Numerical simulation of buoyant flow in a roof of triangular cross section under winter day boundary conditions. Energy Buildings, 33: 753-757.

Correa, S.M., 1987. Fluid flow and heat transfer in incandescent lamps. Int. J. Heat Mass Transfer, 30: 663-672.

De Vahl Davis, G. and L.P. Jones, 1983. Natural Convection in a square cavity: A comparison exercise. Int. Num. Method in Fluids, 3: 227-248.

Gebhart, B., Y. Jaluria, R.L. Mahajan and B. Sammakia, 1988. Buoyancy induced flow and transport. Hemisphere, New York.

Gray, D.D. and A. Giorgini, 1976. The validity of the Boussinesq approximation for liquids and gases. Int. J. Heat Mass Transfer, 19: 545-551.

Holtzman, G.A., R.W. Hill and K.S. Ball, 2000. Laminar natural convection in isosceles triangular enclosures heated from below and symmetrically cooled from above. J. Heat Transfer, 122: 485-491.

Karyakin, Y.E., Y.A. Sokovishin and O.G. Martynenko, 1988. Transient natural convection in triangular enclosures. Int. J. Heat Mass Transfer, 31: 1759-1766.

Kent, E.F., E. Asmaz and S. Ozerbay, 2005. Finite element analysis of steady natural convection in triangular enclosures. 15th National Heat Science Congress, Turkey.

Knupp, P. and S. Steinberg, 1994. Fundamentals of Grid Generation. CRC Press, USA.

Koca, A., 2005. Numerical investigation of heat transfer with laminar natural convection in different roof types. Ph.D Thesis, Firat University, Elazig.

Morsi, Y.S. and S. Das, 2003. Numerical investigation of natural convection inside complex enclosure. Heat Transfer Eng., 24: 30-41.

Moukalled, F. and S. Acharya, 2001. Natural convection in trapezoidal enclosure with offset baffles. J. Thermophysics Heat Transfer, 5: 212-218.

Oosthuizen, P.H. and D. Naylor, 1998. Introduction to convective heat transfer analysis. McGraw-Hill Int. Editions, Singapore.

Ostrach, S., 1988. Natural Convection in Enclosures. J. Heat Transfer, 110: 1175-1190.

Ozisik, M.N., 1994. Finite difference methods in heat transfer. CRC Press, Florida.

Oztop, H.F., 2003. Numerical investigation of flow and heat transfer in asymmetric channels with curvilinear boundaries. Ph.D Thesis, Firat University, Elazig.

Thames, F.C., J.F. Thompson, C.W. Mastin and R.L. Walker, 1977. Numerical solutions for viscous and potential flow about arbitrary two-dimensional bodies using body-fitted Sys. J. Comp. Phys., 24: 245-273.

Tzeng, S.C., J.H. Liou and R.Y. Jou, 2005. Numerical simulation-aided parametric analysis of natural convection in a roof of triangular enclosures. Heat Transfer Eng., 26: 69-79.

Varol, Y., A. Koca and H.F. Oztop, 2007. Natural convection in Gambrel Roofs. Building Environ., 42: 1291-1297.